Collisionless plasma modeling in an arbitrary potential energy distribution

M. W. Liemohn and G. V. Khazanov
Space Sciences Laboratory, National Aeronautical and Space Administration, Marshall Space Flight Center, Mail Code ES-83, Huntsville, Alabama 35812

(Received 26 August 1997; accepted 4 November 1997)

A new technique for calculating a collisionless plasma along a field line is presented. The primary feature of this new ion-exospheric model is that it can handle an arbitrary (including nonmonotonic) potential energy distribution. This was one of the limiting constraints on the existing models in this class, and these constraints are generalized for an arbitrary potential energy composition. The formulation for relating current density to the field-aligned potential as well as formulas for density, temperature, and energy flux calculations are presented for several distribution functions, ranging from a bi-Lorentzian with a loss cone to an isotropic Maxwellian. A comparison of these results with previous models shows that the formulation reduces to the earlier models under similar assumptions. © *1998 American Institute of Physics.* [S1070-664X(98)01502-X]

I. INTRODUCTION

Modeling the behavior of a plasma through the use of the collisionless kinetic equation (Vlasov equation) is a commonly used technique in plasma physics, especially when the primary factors influencing the changes in the distribution function are potential energy structures. It began with exospheric modeling of the Earth's upper atmosphere[1,2] and has broad applications across many disciplines: in near-Earth for describing the hot plasma along inner magnetospheric field lines, high-latitude ionospheric outflows, and other situations involving a field-aligned potential; for rotating planetary magnetospheres to determine the effects of the centrifugal force; expansion into evacuated regions such as the Lunar wake; in astrophysics for describing objects such as pulsars; for modeling the solar wind acceleration region; and in laboratory plasmas to describe collisionless expansion into a vacuum.

For instance, there are many exospheric models describing collisionless flows in solar system plasmas. For example, the trapped radiation in the Earth's magnetic field was first considered with this technique by obtaining a solution using a delta function distribution for the plasma.[3] This was followed by calculations involving more complicated distributions, such as a Maxwellian or bi-Maxwellian[4–15] or a drifting Maxwellian.[16] There is also a rich history of models describing ionospheric outflows and precipitation[5,17–20] as well as solar wind acceleration.[21–23] Several excellent reviews of these applications have been compiled.[24–26]

These collisionless kinetic ion-exosphere models all have the same basic approach of knowing the distribution function at some reference point in a given magnetic field and then mapping this distribution along the field line according to the potential energy structure, whether that potential energy is self-consistently calculated or externally applied. They use one or more of the first few moments of the velocity space distribution function (density, flux, pressure, etc.) either to obtain a self-consistent calculation or to use in conjunction with other results. Also, because of the definitions of the velocity space integration regions, all of these models require that the potential energy distribution along the field line be smooth and monotonic. This was eventually formalized into a set of constraints on the potential energy.[9] In that study, the only potential was the self-consistent electrostatic potential φ, and the constraints on this quantity are limitations on its derivative with respect to the magnetic field B,

$$d\varphi/dB > 0, \tag{1}$$

$$d^2\varphi/dB^2 \leqslant 0. \tag{2}$$

These constraints must be satisfied when the calculation of the moments of the velocity distribution at a point along the field line only includes the parameters (such as potential energy and magnetic field strength) at the end points of the simulation region and those for the local spatial point. It is quite possible, however, to violate these constraints, not only during inner magnetospheric plasma calculations, but also during any collisionless plasma scenario where this type of a solution is appropriate.

The purpose of this study is to develop a generalization of these previous studies to allow for the calculation of a collisionless plasma along a magnetic field line in the presence of an arbitrary potential energy structure. The formulation of the generalized approach is given in Sec. II, followed by a discussion of the implementation of this model for several distribution functions. Two cases of its application will also be discussed, followed by a comparison of this formulation with previous models.

II. THE MODEL

A. Moments of the velocity distribution function

The collisionless nature of the plasma means that the distribution function depends only on the two constants of motion,[8,21] namely, the total energy E,

$$E = \frac{m v_\parallel^2}{2} + \frac{m v_\perp^2}{2} + \Pi \tag{3}$$

and the first adiabatic invariant μ,

$$\mu = \frac{m\nu_\perp^2}{2B}, \tag{4}$$

where m is the plasma particle mass, $\nu_\parallel$ and $\nu_\perp$ are the particle velocities parallel and perpendicular to B, and Π is the total potential energy. This choice is quite beneficial because it removes the spatial dependence in the distribution function f and only the region of integration in $E-\mu$ velocity space changes. The zeroth, first, second, and third moments of the velocity distribution function transformed to these variables from their standard definitions[27] are written as

$$n = \frac{\sqrt{2}\pi B}{m^{3/2}} \int\int \frac{f(E,\mu)}{\sqrt{E-\mu B-\Pi}}\, dE d\mu, \tag{5a}$$

$$\phi = \frac{2\pi B}{m^2} \int\int f(E,\mu) dE d\mu, \tag{5b}$$

$$P_\parallel = \left(\frac{2}{m}\right)^{3/2} \pi B \int\int \sqrt{E-\mu B-\Pi} f(E,\mu) dE d\mu, \tag{5c}$$

$$P_\perp = \frac{\sqrt{2}\pi B^2}{m^{3/2}} \int\int \frac{\mu f(E,\mu)}{\sqrt{E-\mu B-\Pi}}\, dE d\mu, \tag{5d}$$

$$\varepsilon_\parallel = \frac{2\pi B}{m^2} \int\int (E-\Pi) f(E,\mu) dE d\mu, \tag{5e}$$

where (5) has already been integrated over the velocity azimuthal angle. Note that the flow terms must be subtracted out of (5c)–(5e) in order to obtain the thermal portion of these quantities (such as temperature and thermal heat flux).

It should be noted that Π is an arbitrary potential energy structure, and can include an electrostatic potential energy of the form $e\varphi$, a gravitational potential energy of the form $m\Psi_g$, or other potential energies. Also, the squaring of $\nu_\parallel$ in (3) obscures the hemispherical direction of the distribution function. For the integration, then, f must be split into hemispherical descriptions f^+ and f^-. The sign of $\nu_\parallel$ must then be taken into account in (5) such that the functions are subtracted in the flux calculation and summed in the others.

The function $f(E,\mu)$ is then defined at the reference altitude and can be mapped to any point along the field line. The problem which should be solved is the calculation of the region of the $E-\mu$ plane filled by particles for an arbitrary point along the field line. For a given plasma in a given magnetic field, this region is determined by the location of the source of the particles (reference point s_0 on the magnetic field line), and by the conservation laws (3) and (4),

$$\nu_\parallel \geqslant 0, \quad E \geqslant \mu B + \Pi. \tag{6}$$

We will restrict our analysis to the case of a one-to-one relation between distance and field strength, i.e., the magnetic field is a monotonic function of s.

Figure 1 shows the regions of integration for (a) decelerated and (b) accelerated particles when the reference point s_0 is located at $B = B_{\min}$. While the region of integration for the decelerated species is defined simply by the $\nu_\parallel = 0$ line for the local spatial point, the accelerated species requires two lines to define the region. The space below the $s_0\ \nu_\parallel = 0$ line and above the $s_1\ \nu_\parallel = 0$ line is an empty region in velocity space at s_1, created by the acceleration from the potential drop the particles have experienced. The region above the s_0 line yet below the s_1 line are particles that have magnetically mirrored between s_0 and s_1. These regions are also shown in $\nu_\parallel - \nu_\perp$ coordinates in Figs. 1(c) and 1(d), illustrating the region of velocity space at s_1 that maps to s_0 for Figs. 1(a) and 1(b), respectively. In Fig. 1(d), ν_1 corresponds to the offset along the E axis in Fig. 1(b) between the s_0 and s_1 intercepts, ν_2 corresponds to the intersection of the two $\nu_\parallel = 0$ curves, and θ_1 is the s_0 line, algebraically defined by

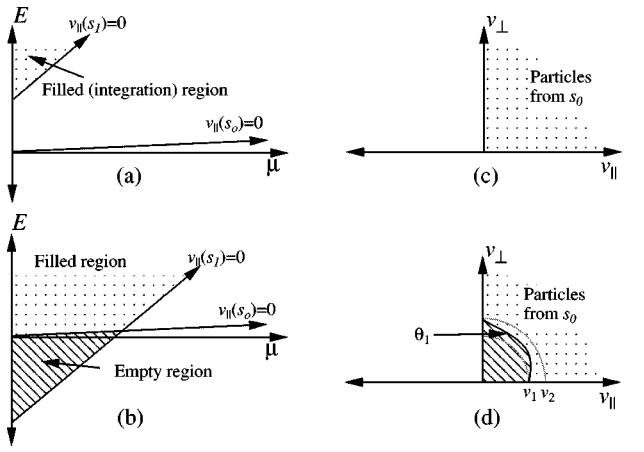

FIG. 1. Regions of integration in $E-\mu$ velocity space for (a) decelerated and (b) accelerated plasma populations at s_1 for a reference point at $B = B_{\min}$. Plots (c) and (d) are the analogous regions in $\nu_\parallel - \nu_\perp$ velocity space. The dotted areas are the regions of integration, the striped areas are empty regions in velocity space at s_1. The distribution function is defined above the $s_0\ \ \nu_\parallel = 0$ line, with no particles below it.

$$\frac{m\nu_1^2}{2} = \Pi_0 - \Pi_1, \quad \frac{m\nu_2^2}{2} = \frac{B_1}{B_1 - B_0}(\Pi_0 - \Pi_1) - \Pi_1,$$

$$\sin^2\theta_1 = \frac{B_1}{B_0}\left(\frac{E-\Pi_0}{E-\Pi_1}\right). \tag{7}$$

For anisotropic trapped plasma in the magnetosphere, this situation corresponds to s_0 at the equatorial plane with the decelerated species being the ions and the accelerated species being the anisotropic electrons.[8]

B. Generalization of the previous constraints

Because the previous collisionless kinetic models include only the calculation of the local and reference point $\nu_\parallel = 0$ lines in their definition of the filled region of velocity space, constraints must be imposed on the the potential energy to ensure that the solution is valid. These were defined above for the electrostatic potential during magnetospheric precipitation, given in (1) and (2). Here, these criteria will be extended for an arbitrary potential energy Π. This will be analyzed using three neighboring points: s_{i-1}, s_i, and s_{i+1}, where i is the spatial grid index. The boundary lines for these points are found from (6),

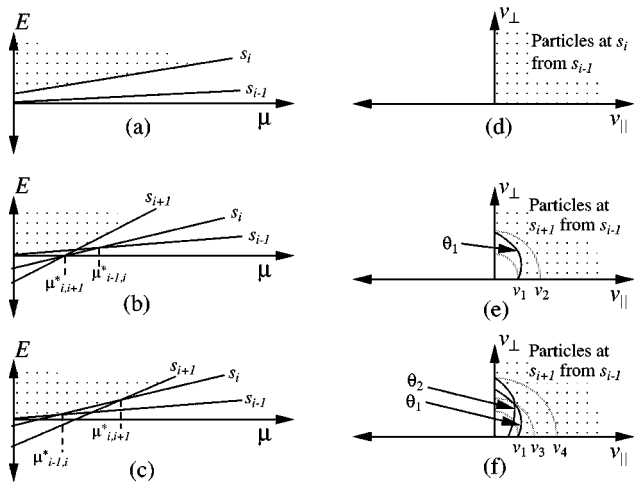

FIG. 2. Schematics of the definition of the filled region of velocity space (dotted area) at s_{i+1} based on three neighboring spatial points. This region is shown for (a) $d\Pi/dB>0$, (b) $d\Pi/dB<0$ with $d^2\Pi/dB^2>0$, and (c) $d\Pi/dB<0$ with $d^2\Pi/dB^2<0$. Plots (d)–(f) are the analogous regions in $\nu_\parallel-\nu_\perp$ space.

$$E=\mu B_\alpha+\Pi_\alpha, \quad \alpha=i-1,i,i+1. \tag{8}$$

Let us begin by supposing that s_{i-1} is the reference point and that $\Pi_{i-1}=0$, but the argument is easily generalized for any three points in the spatial domain. The region above the line $E=\mu B_{i-1}+\Pi_{i-1}$ is therefore filled at s_{i-1}.

In order for the region of integration to be defined by only the $\nu_\parallel=0$ lines from the reference point and the local point, there is just one necessary and sufficient condition that must be met: If the s_{i+1} $\nu_\parallel=0$ line is ever above the reference point (here, s_{i-1}) $\nu_\parallel=0$ line for $\mu>0$, then it must also be above the s_i $\nu_\parallel=0$ line for these μ values. If the potential energy distribution is nonmonotonic, then this condition will not be met for the decelerated species. Because magnetic field and distance are one-to-one, this requirement can be written as follows: The first derivative of the potential energy with respect to the magnetic field must be monotonic throughout the spatial range.

Beginning with this constraint of monotonicity, a second criteria can be derived by considering the intersection of the $\nu_\parallel=0$ lines. The point of intersection for the lines of spatial points s and $s+ds$ (any two adjacent spatial points) is

$$\mu^*=-\frac{d\Pi}{dB}, \quad E^*=\Pi-B\frac{d\Pi}{dB}. \tag{9}$$

If $d\Pi/dB>0$, μ^* is negative and the lines do not cross in the region of definition ($\mu>0$). This is shown in Fig. 2(a) for the case when the minimum magnetic field is at the reference point (e.g., the magnetospheric trap). Figure 2(d) is the transformation of Fig. 2(a) into $\nu_\parallel-\nu_\perp$ coordinates, showing the region of velocity space at s_i that is filled by particles flowing from s_{i-1}. When this derivative is positive, the only criteria on the potential energy for validity of the previous models is monotonicity.

If $d\Pi/dB<0$, then the lines intersect at some $\mu^*>0$. If the points of intersection between lines $i-1$ and i ($\mu^*_{i-1,i}$) and the intersection between i and $i+1$ ($\mu^*_{i,i+1}$) are arranged so that $\mu^*_{i-1,i}<\mu^*_{i,i+1}$ [i.e., $\mu^*(s)<\mu^*(s+ds)$] and $dB/ds<0$, then $d^2\Pi/dB^2>0$. Similarly, if the μ^*'s are arranged so that $\mu^*_{i-1,i}>\mu^*_{i,i+1}$ [i.e., $\mu^*(s)>\mu^*(s)>\mu^*(s+ds)$] and $dB/ds>0$, then again $d^2\Pi/dB^2>0$. This situation is shown in Fig. 2(b), and the filled region is determined by only two lines, from the reference point $(i-1)$ and from the local point (i or $i+1$, but not both). Figure 2(e) is this situation for $\nu_\parallel-\nu_\perp$, with ν_1, ν_2, and θ_1 defined analogously to (7). Therefore, when the first derivative is monotonically negative and the second derivative is positive, then the previous models will be valid.

Finally, if $d\Pi/dB<0$ and either (a) $\mu^*(s)<\mu^*(s+ds)$ with $dB/ds>0$, or (b) $\mu^*(s)>\mu^*(s+ds)$ with $dB/ds<0$, then the second derivative of Π with respect to B will be negative. When this occurs the boundary of the filled region for point $i+1$ will consist of three line segments. For a situation such as that in Fig. 2(c), the boundary is defined first by the s_{i-1} line $E=\mu B_{i-1}+\Pi_{i-1}$ up to $\mu^*_{i-1,i}$, then by the s_i line up to $\mu^*_{i,i+1}$, and finally by the ray $E=\mu B_{i+1}+\Pi_{i+1}$. In general, for these cases the filled region of $E-\mu$ space depends not only on the reference and local point $\nu_\parallel=0$ lines, but also on the potential energy and magnetic field of other (perhaps all) nonlocal points. The $\nu_\parallel-\nu_\perp$ version of this shown in Fig. 2(f). Therefore, the functional dependence of Π with respect to B, then, that ensures the validity of the previous models can be written as two conditions:

$$\frac{d\Pi(B)}{dB}<\frac{d\Pi(B+dB)}{db} \quad \text{for all } B \tag{10a}$$

or

$$\frac{d\Pi(B)}{dB}>\frac{d\Pi(B+dB)}{dB} \quad \text{for all } B \tag{10b}$$

(i.e., $d\Pi/dB$ must be monotonic), and

$$\frac{d^2\Pi}{dB^2}>0 \quad \text{if} \quad \frac{d\Pi}{dB}<0. \tag{11}$$

These constraints must be met for all populations in the calculation. Violation of these constraints leads to other nonlocal $\nu_\parallel=0$ lines entering into the definition of the region of integration for the moments in (5). These extra lines define additional empty regions in velocity space where the particles that would have occupied that region have been reflected before reaching the local spatial point. Although some of the new empty regions in velocity space can be quite small, their proximity to the low-energy range (where f is typically larger) means that they could cause a significant change in the moment calculations.

C. The generalized approach

It is clear that situations can arise that violate these constraints, and the region of integration in $E-\mu$ velocity space requires more than just the $\nu_\parallel=0$ line defined in (6) for the reference point and the local spatial point. Deriving the moments for each possible scenario would be cumbersome, and a general formulation is needed that is applicable for any number of lines defining the integration region at any spatial point along the field line.

Consider the integration region in Fig. 3(a) in $E-\mu$ space and Fig. 3(b) in $\nu_\parallel-\nu_\perp$ space. The shaded area defines

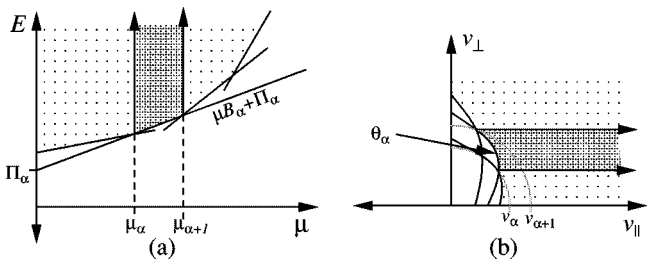

FIG. 3. Integration over a region (dotted area) of (a) $E-\mu$ space and (b) the corresponding $\nu_\parallel-\nu_\perp$ space above an arbitrary $\nu_\parallel=0$ line with arbitrary μ end points.

a region of phase space above an arbitrary $\nu_\parallel=0$ line between two arbitrary end points. While μ_α and $\mu_{\alpha+1}$ can be arbitrarily chosen, they will usually be defined by the intersection of the α line with the $\alpha-1$ and $\alpha+1$ lines, where α is the index ranging through the number of regions comprising the filled velocity space. In $E-\mu$ space, the expressions for the end points and lower line are

$$\mu_\alpha=\frac{\Pi_{\alpha-1}-\Pi_\alpha}{B_\alpha-B_{\alpha-1}}, \quad E_{\min,\alpha}=\mu B_\alpha+\Pi_\alpha \tag{12}$$

and for $\nu_\parallel-\nu_\perp$ they are

$$\frac{m\nu_\alpha^2}{2}=\frac{B_\alpha}{B_\alpha-B_{\alpha-1}}(\Pi_{\alpha-1}-\Pi_\alpha)-\Pi_s,$$

$$\sin^2\theta_\alpha=\frac{B_s}{B_\alpha}\left(\frac{E-\Pi_\alpha}{E-\Pi_s}\right), \tag{13}$$

where the subscript s denotes the current spatial point values. Note that $\alpha=1$ will be at $\mu=0$ ($\nu_\perp=0$) and $\alpha=\alpha_{\max}$ will extend to $\mu\to\infty$ ($\nu_\perp\to\infty$).

Integration over this shaded area (at spatial point s) represents an arbitrary integral of the form

$$I_j(B_\alpha,\Pi_\alpha)=\int_{\mu_\alpha}^{\mu_{\alpha+1}}\left[\int_{E_{\min,\alpha}}^{\infty}F_j(E,\mu)dE\right]d\mu, \tag{14}$$

where F_j is the appropriate kernel from the definition in (5), with $B=B_s$ and $\Pi=\Pi_s$. Note that B_α, Π_α, do not need to be specifically defined to perform this integral, but will eventually be defined by some $\nu_\parallel=0$ line bordering an integration region. Note that these integration boundaries could be defined by any point in the spatial range. The solution over this arbitrary region of $E-\mu$ space is what is needed for a generalization of the previous models. From this, a summation of these integrals can be constructed to obtain the needed moments of the distribution function. These moments can then be used in Maxwell's equations to couple the plasma parameters to the magnetic and electric fields.

III. IMPLEMENTATION

It is now necessary to define the distribution function at the reference altitude. Many functions have been used in the previous studies, particularly the Maxwellian and kappa (Lorentzian) distribution functions. Delta functions in $\nu_\parallel$ and $\nu_\perp$ have also been used, as well as more complex distributions like bi-Maxwellians. The choice of this function primarily depends on the application of interest. A concise table of the common Lorentzian distribution functions and their associated Maxwellian limits for $\kappa\to\infty$ is available.[28]

While the use of any function that satisfies Liouville's theorem is possible, the most general is the bi-Lorentzian loss cone distribution,[28] written in $E-\mu$ velocity space as

$$f=\left(\frac{m}{2\pi}\right)^{3/2}\frac{n_0A_1}{\tau_\parallel^{3/2}}\left(\frac{\mu B_0A_1}{\tau_\parallel}\right)^\sigma \times\frac{\Gamma(\kappa+1)}{\kappa^{\sigma+3/2}\Gamma(\kappa-1/2)\Gamma(\sigma+1)} \times\left(1+\frac{E-\Pi_0+\mu B_0A}{\kappa\tau_\parallel}\right)^{-(\kappa+\sigma+1)}, \tag{15}$$

where $\tau_\parallel=T_\parallel(\kappa-3/2)/\kappa$, $A_1=A+1=T_\parallel/T_\perp$, the i subscript indicates the point of maximum B, and σ quantifies the level of depletion in the loss cone. Various forms of loss cone distributions have been used for the past few decades. The bi-Maxwellian loss cone description of this form was originally used for analyzing plasma wave generation by geomagnetically trapped plasma.[29]

A bi-Maxwellian loss cone distribution using a subtractive Maxwellian instead of a $\nu_\perp$ multiplier was used for a similar application.[30] This subtractive loss cone distribution,

$$f=\left(\frac{m}{2\pi}\right)^{3/2}\frac{n_0A_1\exp\left(-\frac{E-\mu B_0-\Pi_0}{T_\parallel}\right)}{T_\parallel^{3/2}} \times\left\{\delta\exp\left(-\frac{\mu BA_1}{T_\parallel}\right)+\frac{1-\delta}{1-\beta}\left[\exp\left(-\frac{\mu BA_1}{T_\parallel}\right)-\exp\left(-\frac{\mu BA_1}{\beta T_\parallel}\right)\right]\right\} \tag{16}$$

was also used for field-aligned mapping of precipitating particles.[11] This distribution defines a partially filled loss cone, where δ and β range from 0 to 1 and indicate the size and filling ratio of the loss cone at $\nu_\parallel=0$. These two functions are complimentary, and a limit of $\beta\to1$ in (16) reduces to the $\sigma=1$ distribution of (15).

Because the original use of these functions was for dispersion relation calculations, a delta function at the resonant $\nu_\parallel$ was immediately applied, and thus the loss cone was a fixed size in $\nu_\perp$. For this application, however, there is no delta function specifying $\nu_\parallel$, and so the size of the loss cone must vary with $\nu_\parallel$. In fact, the loss cone size depends on the field-aligned distribution of the total potential energy. In this case, then, a more rigorous approach to a loss cone definition is to define the loss cone as the region of integration at $B=B_{\max}$ and define a distribution function to be subtracted from the trapped population in this ''loss cone region'' of velocity space.

Several other distributions are also commonly used. One is the isotropic Lorentzian distribution function,

$$f=\left(\frac{m}{2\pi}\right)^{3/2}\frac{n_0}{\tau^{3/2}}\frac{\Gamma(\kappa+1)}{\kappa^{3/2}\Gamma(\kappa-1/2)}\left(1+\frac{E-\Pi_0}{\kappa\tau}\right)^{-(\kappa+1)}, \tag{17}$$

which has been used for describing the solar wind acceleration region[31,32] as well as near-Earth plasma temperature profiles.[18] The bi-Maxwellian distribution is another function that is often used in collisionless plasma modeling, having the form

$$f=\left(\frac{m}{2\pi}\right)^{3/2}\frac{n_0A_1}{T_\parallel^{3/2}}\exp\left(-\frac{E-\Pi_0+\mu B_0A}{T_\parallel}\right). \tag{18}$$

This function is primarily used for modeling magnetic field-aligned potential energy distributions caused by mirroring anisotropic plasmas,[14,15] and also for rotating planetary magnetospheres.[13,33] A further simplification that is also used extensively is the isotropic Maxwellian distribution function,

$$f=\left(\frac{m}{2\pi}\right)^{3/2}\frac{n_0}{T^{3/2}}\exp\left(-\frac{E-\Pi_0}{T}\right) \tag{19}$$

and was used, for instance, in an ion-exosphere model[5,16,27] and in several recent polar wind outflow studies.[19,20]

In principle, each of these distribution functions can be used in the general model to obtain an analytical form of the velocity moments along a magnetic field line.

IV. APPLICATIONS OF THE MODEL

While there are many applications for mapping a collisionless plasma along a magnetic field in the presence of an arbitrarily complex field-aligned potential distribution, two applications will be discussed here: obtaining a relation between the field-aligned current and potential drop; and quantifying the plasma density and temperature changes along the field line.

A. Current calculations

Finding the relation between the current density and the field-aligned potential has long been a topic of critical importance. The self-consistent formation of a field-aligned potential drop due to field-aligned currents has been considered since the early 1970s,[6,34–37] and there are several good discussions of this topic available.[38,39] From the present model, the final result of the particle flux calculation along the field line will yield a general relation for the current density. The distributions presented in Sec. III can be applied to (5b) using the general integration region limits of 14. As discussed above, the loss cone is best handled by defining the loss cone region of velocity space and subtracting an integration over that area, and so $\sigma=0$ will be used here. For comparison with the formulation of Ref. 11, though, (16) has not been reduced. The resulting general flux integrals are

$$\phi_{\rm gen}^{bi-L}=\frac{n_0}{2}\sqrt{\frac{2\tau_\parallel}{m\pi}}\frac{B}{B_\alpha}\frac{\xi_\kappa^0}{\kappa^{1/2}(\kappa-1)}\frac{A_1}{1+\dfrac{B_0}{B_\alpha}A}\times\left[\left(1+\frac{\mu_1(B_\alpha+B_0A)-\Pi_0+\Pi_\alpha}{\kappa\tau_\parallel}\right)^{-(\kappa-1)}-\left(1+\frac{\mu_2(B_\alpha+B_0A)-\Pi_0+\Pi_\alpha}{\kappa\tau_\parallel}\right)^{-(\kappa-1)}\right], \tag{20}$$

$$\phi_{\rm gen}^{\rm LCM}=\frac{n_0}{2}\sqrt{\frac{2T_\parallel}{\pi m}}\frac{B_s}{B_\alpha}A_1\exp\left(\frac{\Pi_0-\Pi_\alpha}{T_\parallel}\right)\times\left\{\frac{\delta+\left(\dfrac{1-\delta}{1-\beta}\right)}{1+\dfrac{B_0}{B_\alpha}A}\left[\exp\left(-\frac{\mu_1(B_\alpha+AB_0)}{T_\parallel}\right)-\exp\left(-\frac{\mu_2(B_\alpha+AB_0)}{T_\parallel}\right)\right]-\frac{\left(\dfrac{1-\delta}{1-\beta}\right)}{1+\dfrac{B_0}{B_\alpha}\left(\dfrac{A_1}{\beta}-1\right)}\times\left[\exp\left(-\frac{\mu_1[B_\alpha+B_0(A_1/\beta-1)]}{T_\parallel}\right)-\exp\left(-\frac{\mu_2(B_\alpha+B_0[A_1/\beta-1])}{T_\parallel}\right)\right]\right\}, \tag{21}$$

$$\phi_{\rm gen}^{L}=\frac{n_0}{2}\sqrt{\frac{2\tau}{m\pi}}\frac{B}{B_\alpha}\frac{\xi_\kappa^0}{\kappa^{1/2}(\kappa-1)}[(\zeta_1^\alpha)^{-(\kappa-1)}-(\zeta_2^\alpha)^{-(\kappa-1)}], \tag{22}$$

$$\phi_{\rm gen}^{bi-M}=\frac{n_0}{2}\sqrt{\frac{2T_\parallel}{\pi m}}\frac{B_s}{B_\alpha}\frac{A_1}{1+\dfrac{B_0}{B_\alpha}A}\exp\left(\frac{\Pi_0-\Pi_\alpha}{T_\parallel}\right)\times\left[\exp\left(-\frac{\mu_1(B_\alpha+AB_0)}{T_\parallel}\right)-\exp\left(-\frac{\mu_2(B_\alpha+AB_0)}{T_\parallel}\right)\right], \tag{23}$$

$$\phi_{\rm gen}^{M}=\frac{n_0}{2}\sqrt{\frac{2T}{\pi m}}\frac{B_s}{B_\alpha}\exp\left(\frac{\Pi_0-\Pi_\alpha}{T}\right)\times[e^{-\mu_1B_\alpha/T}-e^{-\mu_2B_\alpha/T}], \tag{24}$$

where $\xi_\kappa^0=\Gamma(\kappa+1)/\Gamma(\kappa-1/2)$ and $\zeta_{1,2}^\alpha=1+(\mu_{1,2}B_\alpha+\Pi_\alpha-\Pi_0)/\kappa\tau$.

To obtain the appropriate line segments to integrate above, the potential energy structure must be known on a spatial grid from the reference point to the point of interest. If constraints (10) and (11) are met, then the summation of regions yields the previous relation for the current as a function of the field-aligned potential difference between the local point and the reference point.[6] The potential energy distribution can be more complicated, though, and in this case a calculation along the field line is needed to obtain the $\nu_\parallel=0$ lines defining the region of integration for the flux.

B. Density, temperature, and heat flux

It is often important to determine the local density, temperature, and heat flux of a plasma species, and these can also be obtained by using the functions in Sec. III in the moments in (5) with the limits of (14). This will yield gen-

eral relations for the density, parallel pressure, perpendicular pressure, and heat flux that can be piecewise summed over the appropriate $\nu_\parallel = 0$ lines to obtain the total density or temperature component of the plasma at any given point along the field line. Here, the expressions are presented only for two of the most useful distribution functions: the Lorentzian and bi-Maxwellian. Note that both of these will reduce to the isotropic Maxwellian solution.

The general relations for n, $P_\parallel$, $P_\perp$, and $\epsilon_\parallel$ for (17) are

$$n^L_{\rm gen}=\frac{n_0}{2}\,\xi^1_\kappa\left\{\frac{\left(1-\frac{B}{B_\alpha}\right)^\kappa}{\zeta_0^{\kappa-1/2}}\,H_1(z_1^*,z_2^*)+\frac{H_1(0,z_1)}{\zeta_1^{\kappa-1/2}}-\frac{H_1(0,z_2)}{\zeta_2^{\kappa-1/2}}\right\}, \tag{25}$$

$$P^L_{\parallel,\rm gen}=\frac{n_0\tau}{3}\,\kappa\xi^1_\kappa\left\{\frac{\left(1-\frac{B}{B_\alpha}\right)^\kappa}{\zeta_0^{\kappa-3/2}}\,H_2(z_1^*,z_2^*)+\frac{H_2(0,z_1)}{\zeta_1^{\kappa-3/2}}-\frac{H_2(0,z_2)}{\zeta_2^{\kappa-3/2}}\right\}, \tag{26}$$

$$P^L_{\perp,\rm gen}=P^L_{\parallel,\rm gen}+\frac{n_0\tau}{2}\,\kappa\xi^1_\kappa\left\{\frac{\frac{B}{B_\alpha}\left(1-\frac{B}{B_\alpha}\right)^\kappa}{\zeta_0^{\kappa-3/2}}\,[H_1(z_1^*,z_2^*)+H_2(z_1^*,z_2^*)]+\frac{\mu_1 B}{\kappa\tau}\,\frac{H_1(0,z_1)}{\zeta_1^{\kappa-3/2}}-\frac{\mu_2 B}{\kappa\tau}\,\frac{H_1(0,z_2)}{\zeta_2^{\kappa-3/2}}\right\}, \tag{27}$$

$$\epsilon^L_{\parallel,\rm gen}=(\Pi_\alpha-\Pi)\,\phi^L_{\rm gen}+\frac{n_0}{2}\,\sqrt{\frac{2\tau}{\pi m}}\,\frac{B}{B_\alpha}\,\frac{\xi^0_\kappa}{\kappa^{1/2}(\kappa-1)}\times\left\{\mu_1 B_\alpha(\zeta_1^\alpha)^{-(\kappa-1)}+\mu_2 B_\alpha(\zeta_2^\alpha)^{-(\kappa-1)}+\frac{2\kappa\tau}{\kappa-2}\,[(\zeta_1^\alpha)^{-(\kappa-2)}-(\zeta_2^\alpha)^{-(\kappa-2)}]\right\}, \tag{28}$$

where $\xi^1_\kappa=\xi^0_\kappa/\Gamma(3/2)$, the new ζ terms are

$$\zeta_0=1-\frac{B}{B_\alpha}+\frac{\Pi-\Pi_0+\frac{B}{B_\alpha}\,(\Pi_0-\Pi_\alpha)}{\kappa\tau},$$

$$\zeta_{1,2}=1+\frac{\mu_{1,2}B+\Pi-\Pi_0}{\kappa\tau}, \tag{29}$$

the z limits are

$$z_{1,2}=\frac{\zeta_{1,2}}{1+\frac{\mu_{1,2}B_\alpha+\Pi_\alpha-\Pi_0}{\kappa\tau}},$$

$$z^*_{1,2}=\frac{\zeta_0}{\left(1+\frac{B}{B_\alpha}\right)\left(1+\frac{\mu_{1,2}B+\Pi-\Pi_0}{\kappa\tau}\right)}, \tag{30}$$

and the two H functions are the integrals

$$H_1(u_1,u_2)=\int_{u_1}^{u_2}t^{\kappa-3/2}(1-t)^{1/2}dt,$$

$$H_2(u_1,u_2)=\int_{u_1}^{u_2}t^{\kappa-5/2}(1-t)^{3/2}dt, \tag{31}$$

which can be readily written in series form.[40]

The general relations for n, $P_\parallel$, $P_\perp$, and $\epsilon_\parallel$ for (18) are

$$n^{bi-M}_{\rm gen}=\frac{n_0}{2}\,\frac{A_1}{1+A\,\frac{B_0}{B_s}}\,\exp\left(\frac{\Pi_0-\Pi_s}{T_\parallel}\right)\times\left\{\mathrm{erfc}(\sqrt{x_1})\exp\left(-\frac{\mu_1(B_s+AB_0)}{T_\parallel}\right)-\mathrm{erfc}(\sqrt{x_2})\exp\left(-\frac{\mu_2(B_s+AB_0)}{T_\parallel}\right)+G_1(y)\exp\left(\frac{B_s+AB_0}{B_\alpha-B_s}\,\frac{\Pi_\alpha-\Pi_s}{T_\parallel}\right)\right\}, \tag{32}$$

$$P^{bi-M}_{\parallel,\rm gen}=n^{bi-M}_{\rm gen}T_\parallel+\frac{1}{2}\,n_0T_\parallel\,\frac{A_1}{1+A\,\frac{B_0}{B_s}}\,G_3(y)\times\exp\left(\frac{\Pi_0-\Pi_s}{T_\parallel}+\frac{B_s+AB_0}{B_\alpha-B_s}\,\frac{\Pi_\alpha-\Pi_s}{T_\parallel}\right), \tag{33}$$

$$P^{bi-M}_{\perp,\rm gen}=\frac{P^{bi-M}_{\parallel,\rm gen}}{1+A\,\frac{B_0}{B_s}}+\frac{n_0T_\parallel}{2}\,\exp\left(\frac{\Pi_0-\Pi_s}{T_\parallel}\right)\,\frac{A_1}{\left(1+A\,\frac{B_0}{B_s}\right)^2}\times\left\{\frac{\mu_1(B_s+AB_0)}{T_\parallel}\,\mathrm{erfc}(\sqrt{x_1})\times\exp\left(-\frac{\mu_1(B_s+AB_0)}{T_\parallel}\right)-\frac{\mu_2(B_s+AB_0)}{T_\parallel}\times\mathrm{erfc}(\sqrt{x_2})\exp\left(-\frac{\mu_2(B_s+AB_0)}{T_\parallel}\right)+\frac{\Pi_\alpha-\Pi_s}{T_\parallel}\,G_2(y)\exp\left(\frac{B_s+AB_0}{B_\alpha-B_s}\,\frac{\Pi_\alpha-\Pi_s}{T_\parallel}\right)\right\}, \tag{34}$$

$$\epsilon_{\parallel,\mathrm{gen}}^{bi-M}=\left(\Pi_\alpha-\Pi+T_\parallel\left[1+\left(\frac{B_\alpha}{B_\alpha+B_0A}\right)^2\right]\right)\phi_{\mathrm{gen}}^{bi-M}+\frac{n_0}{2}\sqrt{\frac{2T_\parallel}{\pi m}}\,e^{(\Pi_0-\Pi_\alpha)/T_\parallel}\,\frac{BA_1B_\alpha}{B_\alpha+B_0A}\times\left[\mu_1\,\exp\left(-\frac{\mu_1(B_\alpha+B_0A)}{T_\parallel}\right)-\mu_2\,\exp\left(-\frac{\mu_2(B_\alpha+B_0A)}{T_\parallel}\right)\right],\tag{35}$$

where x and y are

$$x_{1,2}=\frac{\mu_{1,2}(B_\alpha-B_s)+\Pi_\alpha-\Pi_s}{T_\parallel},\quad y=\frac{B_\alpha+AB_0}{B_\alpha-B_s}\tag{36}$$

and the three G functions are defined as

$$G_1(y)=\begin{cases}y=0: & G_1=\dfrac{2}{\sqrt{\pi}}\left[\sqrt{x_1}-\sqrt{x_2}\right]\\ y>0: & G_1=\dfrac{1}{\sqrt{y}}\left[\mathrm{erf}(\sqrt{yx_1})-\mathrm{erf}(\sqrt{yx_2})\right]\\ y<0: & G_1=\dfrac{2}{\sqrt{-y\pi}}\left[e^{-yx_1}D(\sqrt{-yx_1})-e^{-yx_2}D(\sqrt{-yx_2})\right]\\ y\to\infty: & G_1=0\end{cases},\tag{37}$$

$$G_2(y)=\begin{cases}y=0: & G_2=\dfrac{2y}{\sqrt{\pi}}\left(\dfrac{B_s+AB_0}{B_\alpha+AB_0}\right)\left[\sqrt{x_1}-\sqrt{x_2}\right]\\ y>0: & G_2=\sqrt{y}\left(\dfrac{B_s+AB_0}{B_\alpha+AB_0}\right)\left[\mathrm{erf}(\sqrt{yx_1})-\mathrm{erf}(\sqrt{yx_2})\right]\\ y<0: & G_2=-2\sqrt{\dfrac{-y}{\pi}}\left(\dfrac{B_s+AB_0}{B_\alpha+AB_0}\right)\left[e^{-yx_1}D(\sqrt{-yx_1})-e^{-yx_2}D(\sqrt{-yx_2})\right]\\ y\to\infty: & G_2=0\end{cases},\tag{38}$$

$$G_3(y)=\begin{cases}y=0: & G_3=\dfrac{2y}{3\sqrt{\pi}}\left(\dfrac{B_s+AB_0}{B_\alpha+AB_0}\right)\left[x_1^{3/2}-x_2^{3/2}\right]\\ y>0: & G_3=\left(\dfrac{B_s+AB_0}{B_\alpha+AB_0}\right)\left[\dfrac{\mathrm{erf}(\sqrt{yx_1})}{\sqrt{y}}-\dfrac{\mathrm{erf}(\sqrt{yx_2})}{\sqrt{y}}-\sqrt{\dfrac{x_1}{\pi}}\,e^{-yx_1}+\sqrt{\dfrac{x_2}{\pi}}\,e^{-yx_2}\right]\\ y<0: & G_3=\dfrac{\left(\dfrac{B_s+AB_0}{B_\alpha+AB_0}\right)}{\sqrt{\pi}}\left[e^{-yx_1}\left(\dfrac{D(\sqrt{-yx_1})}{\sqrt{-y}}-\sqrt{x_1}\right)-e^{-yx_2}\left(\dfrac{D(\sqrt{-yx_2})}{\sqrt{-y}}-\sqrt{x_2}\right)\right]\\ y\to\infty: & G_3=0\end{cases}.\tag{39}$$

These equations can be used for many applications, such as polar wind outflows, magnetospheric precipitation, or trapped plasma anisotropies.

V. COMPARISON WITH PREVIOUS MODELS

By applying these general formulas for the regions of integration satisfying the constraints of previous ion-exospheric models, the original equations from those studies can be obtained, showing the generality of this new model.

To obtain the formulation of Ref. 27, integration regions consistent with their model must be taken. This includes assuming that the generalized constraints (10) and (11) are met and using a Maxwellian distribution function. For outflowing particles, for example, the source region is above the ionospheric boundary $v_\parallel=0$ line. Accelerated populations will always escape and the integration is always defined by this boundary line. Plasma populations decelerated by a potential barrier can be divided into two groups: ballistic and escap-

ing. Calculation of the ballistic particle parameters is then an integration above the local point's $\nu_\parallel = 0$ line and below the $s_\infty \nu_\parallel = 0$ line while remaining above the s_0 line, and the escaping particle integrations are above the s_∞ and s_0 lines. The equations for this escaping population of a decelerated population can then be written out by applying (24) and (32)–(35) with $A=0$ for each of these lines and summing the result, obtaining

$$n = n_0 \exp\left(\frac{\Pi_0-\Pi}{T}\right)\left\{ \operatorname{erfc}\left(\sqrt{\frac{\Pi_\infty-\Pi}{T}}\right) - \sqrt{\frac{B_0-B}{B_0}}\exp\left(\frac{B}{B_0-B}\frac{\Pi_0-\Pi}{T}\right)\operatorname{erfc}\left(\sqrt{\frac{B}{B_0-B}\,x}\right)\right.$$
$$+\frac{2}{\sqrt{\pi}}\sqrt{\frac{B-B_\infty}{B_\infty}}\exp\left(\frac{B}{B_\infty-B}\frac{\Pi_\infty-\Pi}{T}\right)\left[\exp\left(\frac{B_\infty}{B-B_\infty}\frac{\Pi_\infty-\Pi}{T}\right)D\left(\sqrt{\frac{B_\infty}{B-B_\infty}\frac{\Pi_\infty-\Pi}{T}}\right)\right.$$
$$\left.\left.-\exp\left(\frac{B_\infty}{B-B_\infty}x\right)D\left(\sqrt{\frac{B_\infty}{B-B_\infty}x}\right)\right]\right\}, \tag{40}$$

$$\phi = n_0\sqrt{\frac{2T}{\pi m}}\frac{B}{B_\infty}\exp\left(\frac{\Pi_0-\Pi_\infty}{T}\right)\left\{1-\frac{B_0-B_\infty}{B_0}\exp\left(\frac{B_\infty}{B_0-B_\infty}\frac{\Pi_0-\Pi_\infty}{T}\right)\right\}, \tag{41}$$

$$P_\parallel = nT + n_0T\exp\left(\frac{\Pi_0-\Pi}{T}\right)\left\{\exp\left(\frac{B}{B_0-B}\frac{\Pi_0-\Pi}{T}\right)\frac{B}{B_0}\left[\sqrt{\frac{B_0-B}{B_0}}\operatorname{erfc}\left(\sqrt{\frac{B_0}{B_0-B}x}\right)+\sqrt{\frac{x}{\pi}}\exp\left(-\frac{B_0}{B_0-B}x\right)\right]\right.$$
$$-\exp\left(\frac{B}{B_\infty-B}\frac{\Pi_\infty-\Pi}{T}\right)\frac{1}{\sqrt{\pi}}\frac{B}{B_\infty}\left[\exp\left(\frac{B_\infty}{B-B_\infty}x\right)\left(\sqrt{\frac{B-B_\infty}{B_\infty}}D\left(\sqrt{\frac{B_\infty}{B-B_\infty}x}\right)-\sqrt{x}\right)-\exp\left(\frac{B_\infty}{B-B_\infty}\frac{\Pi_\infty-\Pi}{T}\right)\right.$$
$$\left.\left.\times\left(\sqrt{\frac{B-B_\infty}{B_\infty}}D\left(\sqrt{\frac{B_\infty}{B-B_\infty}\frac{\Pi_\infty-\Pi}{T}}\right)-\sqrt{\frac{\Pi_\infty-\Pi}{T}}\right)\right]\right\}, \tag{42}$$

$$P_\perp = P_\parallel + n_0T\exp\left(\frac{\Pi_0-\Pi}{T}\right)\left\{\frac{\Pi_0-\Pi}{T}\exp\left(\frac{B}{B_0-B}\frac{\Pi_0-\Pi}{T}\right)\frac{B}{B_0}\sqrt{\frac{B}{B_0-B}}\operatorname{erfc}\left(\sqrt{\frac{B}{B_0-B}x}\right)\right.$$
$$+\frac{\Pi_\infty-\Pi}{T}\exp\left(\frac{B}{B_\infty-B}\frac{\Pi_\infty-\Pi}{T}\right)\frac{B}{B_\infty}\sqrt{\frac{B_\infty}{B-B_\infty}}\left[\exp\left(\frac{B_\infty}{B-B_\infty}\frac{\Pi_\infty-\Pi}{T}\right)D\left(\sqrt{\frac{B_\infty}{B-B_\infty}\frac{\Pi_\infty-\Pi}{T}}\right)\right.$$
$$\left.\left.-\exp\left(\frac{B_\infty}{B-B_\infty}x\right)D\left(\sqrt{\frac{B_\infty}{B-B_\infty}x}\right)\right]\right\}, \tag{43}$$

$$\epsilon_\parallel = n_0T\sqrt{\frac{2T}{\pi m}}\frac{B}{B_\infty}\exp\left(\frac{\Pi_0-\Pi_\infty}{T}\right)\left\{2+\frac{\Pi_\infty-\Pi}{T}-\left[\frac{B_\infty}{B_0}\frac{\Pi_0-\Pi_\infty}{T}+\frac{B_0-B_\infty}{B_0}\left(2+\frac{\Pi_\infty-\Pi}{T}\right)\right]\exp\left(\frac{B_\infty}{B_0-B_\infty}\frac{\Pi_0-\Pi_\infty}{T}\right)\right\}, \tag{44}$$

where

$$x = \frac{B_0-B}{B_0-B_\infty}\frac{\Pi_\infty-\Pi_0}{T}+\frac{\Pi_0-\Pi}{T}. \tag{45}$$

These are the same equations as (17)–(19) of Ref. 27, where their shorthand notations can be written in terms of our variables as

$$p=\frac{B_0-B}{B_0},\quad \sigma=\frac{B-B_\infty}{B_\infty},\quad q=\frac{\Pi-\Pi_0}{T},$$
$$V_\infty^2=\frac{\Pi_\infty-\Pi}{T},\quad X^2=x. \tag{46}$$

The other classes of particles discussed by them can also be compared with this model by applying (24) and (32)–(35) for the appropriate regions and converting the two sets of equations to a common set of variables. It can be shown that the results are the same. It can also be shown that application of (22) and (25)–(28) for these same integration regions yield the results of Ref. 18, although the heat flux of that study, their Equation (29), does not exactly reduce to the corresponding equations of Ref. 27, and this has been corrected by those authors.[41]

The same approach can be used to compare this formulation with other models. Because only the local spatial point in defining the integration region was taken into account in the results of Ref. 15, it is only necessary to apply (32) once above the local point's $\nu_\parallel = 0$ line, with the μ end points at zero and infinity. As mentioned in that study, this implies some scattering mechanism is filling in the low-energy holes

in the accelerated population distributions. Although the scattering is inconsistent with the use of Vlasov's equation, the new model is still capable of reproducing their results. A similar assumption was probably made in Ref. 13, because the formulation is the same except for a more generalized potential energy. For this comparison, $\Pi = \pm e\phi$, and the solution gives unity for everything inside the curly brackets of (32), making the moments proportional to an anisotropy factor and an exponential term. Equating the accelerated and decelerated population densities yields their explicit formula for the field-aligned potential,

$$e\phi = \frac{T_{\|i}T_{\|e}}{T_{\|i}+T_{\|e}} \ln\left(\frac{1+\left(\frac{B_s}{B_0}-1\right)\Big/ A_{1e}}{1+\left(\frac{B_s}{B_0}-1\right)\Big/ A_{1i}} \right). \tag{47}$$

Another result of these studies is a relation for $T_\perp$, and application of the above-mentioned integration limits to (34) will give this $T_\perp$ formula. In general, though, a more complicated formula will arise that depends on a summation of integrals.

Two integrals, one above $E=0$ and one above the local $v_\|=0$ line when it crosses the first line, are needed to reproduce the density formula of Ref. 14. Again, the introduction of the Heaviside step function implies that some process is scattering the accelerated particles and partially filling the low-energy hole. This step function in their results causes the multiplying term to appear for the anisotropic electrons due to the $E=0$ line integration, while the ions will have a formulation like that of Ref. 15.

The results in Sec. IV A can also be checked against previous models. To obtain the parallel current formula in Ref. 6, the region of integration for (23) must be above the $v_\|=0$ lines for the magnetospheric and ionospheric boundaries, with the populations being only ionospheric (i) and plasma sheet (m) electrons. Setting the integration regions to the end point $v_\|=0$ lines (count only those particles not being reflected) and multiplying by the charge, this summation will yield

$$\begin{aligned} j_\| = eB_s\Bigg\{ & \frac{n_i}{B_m}\sqrt{\frac{T_i}{2\pi m}}\left[\exp\left(-\frac{\Pi_m-\Pi_i}{T} \right) \right. \\ & \left. -\left(1-\frac{B_m}{B_i}\right)\exp\left(-\frac{\Pi_m-\Pi_i}{T}\frac{B_i}{B_i-B_m} \right) \right] \\ & -\frac{n_m}{B_m}\sqrt{\frac{T_m}{2\pi m}}\left[1-\left(1-\frac{B_m}{B_i}\right) \right. \\ & \left. \times\exp\left(-\frac{\Pi_m-\Pi_i}{T}\frac{B_m}{B_i-B_m} \right) \right] \Bigg\}, \end{aligned} \tag{48}$$

which is the result previously obtained. As a final comparison, the field-aligned current for the loss cone distribution in Ref. 11 can be derived from this model in a similar manner to (48) by using (21) instead of (23) for magnetospheric particles only. This yields

$$j_\| = en_m\sqrt{\frac{T_\|}{2\pi m}}\frac{B_i}{B_m}\left\{ 1-\frac{\delta e^{-w}}{1+b}-\frac{1-\delta}{1-\beta} \times\left[\frac{e^{-w}}{1+b}-\frac{\beta^2 e^{-w/\beta}}{\beta+b} \right] \right\}, \tag{49}$$

which is his result with $r=0$, $b=A_1B_m/(B_i-B_m)$, and $w=(\Pi_m-\Pi_i)/T_\|$. Although the previous results can be obtained from this new model, a more general approach to loss cone distribution calculations was discussed above (Sec. III).

VI. SUMMARY

While the existing ion-exospheric models of calculating moments of a collisionless plasma by applying Liouville's theorem to solve the Vlasov equation are valid and useful, their validity is limited by at the very least the constraints on the distribution of the potential with respect to the magnetic field strength given in (10) and (11). These constraints can be violated by common geophysical situations by the inclusion of one or more other potential energies or plasma species.

To address this problem, we have developed a generalization to the previous models for the solution of the self-consistent potential energy with an arbitrary field-aligned distribution, including any number of nonmonotonicities. The formulas for a wide range of distribution functions at the reference point, from a loss cone bi-Lorentzian down to an isotropic Maxwellian distribution, are derived and presented. It can handle an arbitrary definition of the reference point, even multiple reference points for different plasma species, and can handle widely varying plasma populations and distribution functions for those populations simultaneously. Also, it can be used for any collisionless plasma situation, where a field-aligned solution is needed. Application of this exospheric model to determining the relationship between field-aligned current and potential difference has been discussed, as well as the calculation of other moments of the distribution function. It has discussed that the solution can depend on all of the spatial points above and below a given spatial point, and that the solution must be iterated to convergence. It was also demonstrated that this new general formulation reduces to the results of the previous models under the same constraints.

ACKNOWLEDGMENTS

This work was funded by the National Science Foundation under Grants No. ATM-9523699 and No. ATM-9710326. M.W.L. held a National Research Council Resident Research Associateship at the National Aeronautics and Space Administration Marshall Space Flight Center while this work was performed.

[1] J. H. Jeans, *The Dynamical Theory of Gases*, 4th ed. (Dover, New York, 1954), Chap. 15.
[2] L. Spitzer, Jr., in *The Atmospheres of the Earth and Planets*, 2nd ed. (University of Chicago Press, Chicago, 1952), p. 211.
[3] H. Alfvén and C.-G. Fälthammar, *Fundamental Principles* (Oxford University Press, London, 1963).
[4] A. Eviatar, A. M. Lenchek, and S. F. Singer, Phys. Fluids **7**, 1775 (1964).
[5] J. Lemaire and M. Scherer, Planet. Space Sci. **18**, 103 (1970).
[6] S. Knight, Planet. Space Sci. **21**, 741 (1973).

[7]J. Lemaire and M. Scherer, Planet. Space Sci. **21**, 281 (1973).
[8]E. C. Whipple, J. Geophys. Res. **82**, 1525 (1977).
[9]Y. T. Chiu and M. Schulz, J. Geophys. Res. **83**, 629 (1978).
[10]Y. Serizawa and T. Sato, Geophys. Res. Lett. **11**, 595 (1984).
[11]K. Stasiewicz, Planet. Space Sci. **33**, 591 (1985).
[12]W. Lennartsson, Laser Part. Beams **5**, 315 (1987).
[13]T. S. Huang and T. J. Birmingham, J. Geophys. Res. **97**, 1511 (1992).
[14]R. H. Miller and G. V. Khazanov, Geophys. Res. Lett. **20**, 1331 (1993).
[15]R. C. Olsen, L. J. Scott, and S. A. Boardsen, J. Geophys. Res. **99**, 2191 (1994).
[16]J. Lemaire and M. Scherer, Phys. Fluids **15**, 760 (1972).
[17]H. Washimi and I. Katanuma, Geophys. Res. Lett. **13**, 897 (1986).
[18]V. Pierrard and J. Lemaire, J. Geophys. Res. **101**, 7923 (1996).
[19]G. V. Khazanov, M. W. Liemohn, and T. E. Moore, J. Geophys. Res. **102**, 7509 (1997).
[20]G. R. Wilson, G. V. Khazanov, and J. L. Horwitz, Geophys. Res. Lett. **24**, 1183 (1997).
[21]J. W. Chamberlain, Astrophys. J. **131**, 47 (1960).
[22]E. Jensen, Astrophys. Norv. **8**, 99 (1963).
[23]F. L. Scarf, J. H. Wolfe, and R. W. Silva, J. Geophys. Res. **72**, 993 (1967).
[24]J. Lemaire and M. Scherer, Rev. Geophys. Space Phys. **11**, 427 (1973).
[25]T. M. Donahue, Rev. Geophys. Space Phys. **9**, 1 (1971).
[26]M. Maksimovic, V. Pierrard, and J. F. Lemaire, Astron. Astrophys. **324**, 725 (1997).
[27]J. Lemaire and M. Scherer, Phys. Fluids **14**, 1683 (1971).
[28]D. Summers and R. M. Thorne, Phys. Fluids B **3**, 1835 (1991).
[29]R. A. Dory, G. E. Guest, and E. G. Harris, Phys. Rev. Lett. **14**, 131 (1965).
[30]M. Ashour-Abdalla and C. F. Kennel, J. Geophys. Res. **83**, 1531 (1978).
[31]J. D. Scudder, Astrophys. J. **389**, 299 (1992).
[32]J. D. Scudder, Astrophys. J. **398**, 319 (1992).
[33]J. Lemaire, Planet. Space Sci. **24**, 975 (1976).
[34]J. Lemaire and M. Scherer, Planet. Space Sci. **22**, 1485 (1974).
[35]M. Fridman and J. Lemaire, J. Geophys. Res. **85**, 664 (1980).
[36]J. Lemaire and M. Scherer, Ann. Geophys. (France) **1**, 91 (1983).
[37]V. Pierrard, J. Geophys. Res. **101**, 2669 (1996).
[38]L. R. Lyons and D. J. Williams, *Quantitative Aspects of Magnetospheric Physics* (Reidel, Boston, 1984), p. 109.
[39]D. P. Stern, Rev. Geophys. **34**, 1 (1996).
[40]For instance, using equations 2.260 and 2.261 from I. S. Gradshteyn and I. M. Ryzhik, *Table of Integrals, Series, and Products*, 5th ed., edited by A. Jeffrey (Academic, San Diego, 1994), p. 98.
[41]V. Pierrard and J. Lemaire, J. Geophys. Res. **102** (in press, 1998).